JOURNAL OF CATALYSIS 48, 1–7 (1977)

Catalytic Activity of Transition Metal Ion Exchanged Y Zeolites in the Reduction of Nitric Oxide with Ammonia

TETSURO SEIYAMA, TSUYOSHI ARAKAWA, TOSHIO MATSUDA,
YUSAKU TAKITA, AND NOBORU YAMAZOE

*Department of Materials Science and Technology, Faculty of Engineering,
Kyushu University, Higashi-ku, Fukuoka, 812 Japan*

Received December 8, 1975; revised March 1, 1977

Catalytic reduction of nitric oxide with ammonia was studied over transition metal ion exchanged Y zeolites (Me–Y). Among various catalysts used, Cu(II)–Y was found to be of particular interest, exhibiting low temperature activity coupled with an unusual activity–temperature profile. In the binary metal ion exchanged systems, where one of the component ions was fixed as Cu(II), promoting effects of the second ionic species were observed. This seems to be correlated with the oxidation potential of the second ion. Both NH_3 and NO were adsorbed considerably on Cu(II)–Y, suggesting that the NO–NH_3 reaction proceeds between adsorbed molecules. Further, from the measurement of reaction kinetics, the mechanism was proposed to be a Langmuir–Hinshelwood type of reaction of NO and NH_3 coordinated to Cu(II) ions.

INTRODUCTION

The removal of nitrogen oxides from exhaust streams is a subject of current importance. As for nitric oxide removal, the most effective way is to reduce it with appropriate agents over catalysts. Various combinations of metal or metal oxide catalysts and reducing agents have already been explored (*1–5*). However, little is known about the catalytic activity of transition metal ion exchanged zeolites in the NO reduction reaction. In this paper we report on the reduction of NO with ammonia over such catalysts.

EXPERIMENTAL METHODS

Transition metal ion exchanged Y zeolites (Me–Y) were prepared by treating Linde Na–Y zeolite with aqueous solutions of metal sulfates. After the exchange the samples were filtered, washed with distilled water and dried at 100°C for 12 hr. The degree of ion exchange was determined by chelatometric titration of residual metal ion in the filtrate. In the case of binary cation exchanged zeolite, (Me_1, Me_2)–Y, the second component ion was exchanged consecutively after the exchange of the first component ion. The exchange level of each component was determined by X-ray fluorimetry using calibration curves obtained with single component exchanged samples. X-Ray powder diffraction patterns of zeolite samples measured before and after the exchange confirmed that there was no detectable loss in crystallinity caused by exchange.

The catalytic reaction was carried out in a fixed bed flow reactor under atmospheric pressure. The gaseous mixture of NO and NH_3, diluted with helium, was passed through the catalyst bed at a fixed contact time, usually $1\ g\cdot s/cm^3$. The gas composition was analyzed before and after the reaction by gas chromatography using the

ISSN 0021-9517

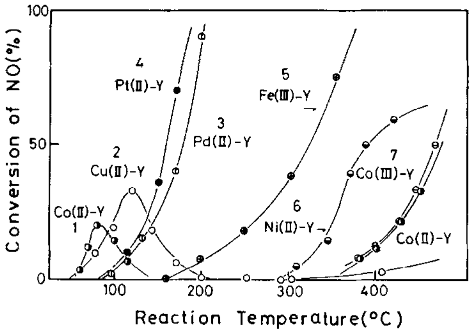

FIG. 1. Catalytic activity of Me–Y for the NO–NH_3 reaction. Flow rate: NO, 1.8; NH_3, 1.2; He, 57 cm^3/min. Contact time, 1 g·s/cm^3. Exchange level of metal ion is as follows. (1) Co(II), 70%; (2) Cu(II), 68%; (3) Pd(II), 48%; (4) Pt(II), 52%; (5) Fe(III), 75%; (6) Ni(II), 80%; (7) Co(III), 95%.

following column packings; Molecular sieve 13 X for N_2 and NO, Porapak Q for N_2O, and Chromosorb 104 for NH_3.

The adsorption of NH_3 and NO on the catalyst samples was measured gravimetrically with a silica spring balance. Prior to the adsorption, samples were dehydrated *in vacuo* at 400°C for several hours.

RESULTS AND DISCUSSION

NO–NH_3 reaction over Me–Y

The catalytic activity of various Me–Y catalysts for the NO–NH_3 reaction was tested over a wide range of temperature. The fraction of NO converted at a fixed contact time was taken as a measure of the catalytic activity. Figure 1 shows the conversion of NO at various temperatures. The reaction products were N_2, N_2O, and H_2O. At lower conversion levels, the selectivity for N_2 was 60–80% in all the cases as listed in Table 1.

As shown in Fig. 1, the catalytic activity of Me–Y as well as its temperature dependence differs greatly depending on the cationic species exchanged in zeolite. Unexchanged catalyst, Na–Y, exhibited no detectable catalytic activity under the reaction conditions. The exchanged catalysts are conveniently classified into two groups. The first group consists of those which show a monotonic increase in catalytic activity with increasing temperature. Pt(II), Pd(II), Fe(III), Ni(II), and Co(III) exchanged in Y zeolites belong to this group. Pt(II)-Y and Pd(II)-Y, known to be active in many other catalytic reactions, were highly active also in this case, whereas Fe(III)-Y, Ni(II)-Y, and Co(III)-Y were much less active. The activity order was

$$\mathrm{Pt(II)\text{-}Y} > \mathrm{Pd(II)\text{-}Y} \gg \mathrm{Ni(II)\text{-}Y} > \mathrm{Co(III)\text{-}Y}.$$

More interesting, however, was the second group consisting of Cu(II)-Y and Co(II)-Y, both of which were active at lower temperatures with unique temperature dependences. In the case of Cu(II)-Y, the catalytic activity, detectable at a temperature as low as 50°C, showed a bell-shaped dependence upon temperature, with the activity maximum appearing at about 120°C. Above 300°C, it again increased, though only gradually. This temperature dependence was completely reversible over Cu(II)-Y. Along with this activity change, the color of the catalyst was found to change with temperature. That is, the color, blue at about 100°C, faded out gradually on raising temperature, becoming white at about 200°C. This strongly indicates that Cu(II) is reduced to Cu(I) in this temperature range. Williamson *et al.* (*16*) and Herman *et al.* (*17*) reported that Cu(II)-Y was reduced to Cu(I) in H_2 or NH_3 at 200 and 180°C, respectively. Such a reduction of Cu(II) in the present study was in fact confirmed by separate esr measurement. Therefore, it is highly probable that the bell-shaped activity profile observed is correlated with the change of the oxidation state of the copper ion, though a quantitative correlation remains to be confirmed.

A seemingly similar behavior was observed with a freshly prepared Co(II)-Y, when it was examined under stepwise temperature increase. In this case, however, the catalytic reaction was accompanied by an irreversible deterioration of catalytic activity and once it deteriorated the activity was not restored even when temperature was lowered. The color change of the catalyst from pink to brown suggested the oxidation of Co(II) to Co(III). After the deactivation, the catalyst was confirmed to follow the same temperature dependence as Co(III)-Y, which exhibited activity only at higher temperatures.

As mentioned above, only Cu(II) was associated with the reversible bell-shaped temperature dependence of catalytic activity. Since the temperature dependence was rather unusual, we examined whether it was commonly observed with other faujasite group zeolites. As a result, Cu(II) exchanged Linde 13 X and 5 A were studied and were found to show the same trend (Fig. 2). Specific activities per Cu(II) at the activity maxima (at 120°C) were 19.6, 20.3, and 4.8 mmol NO/min for Cu(II)-Y, Cu(II)-X, and Cu(II)-A, respectively. Considering that zeolites Y and X have cavities of larger aperture (7.4 Å) than that of zeolite A (4.2 Å), the activity sequence, Y $\simeq$ X > A, may be attributed to the difference in molecular diffusibility within the zeolites. Similar examination was extended to the Cu(II) form of the cation exchange resins, Amberlite 200 C and Amberlyst 15, but neither showed significant catalytic activity below 110°C, probably due to the difficulty of transporting reactant gases through the resins.

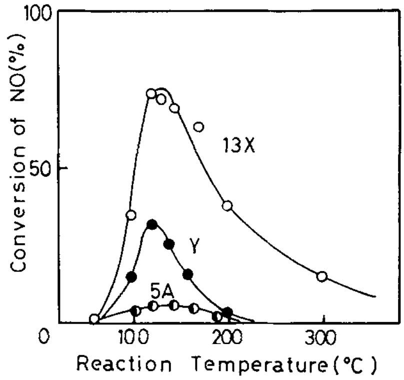

FIG. 2. Catalytic activities of Cu(II) exchanged faujasite group zeolites for the NO–NH_3 reaction. Amounts of Cu(II) exchanged in zeolites 13 X, Y, and 5 A were 3.03, 1.28, and 1.05 mmol/g of catalyst, respectively.

TABLE 1

Selectivity for N_2 in the NO–NH_3 Reaction

Catalyst	Reaction temp (°C)	Selectivity N_2 (%)	Conversion of NO (%)
Pt(II)-Y	135	57	21.1
Pd(II)-Y	143	70	15.5
Co(II)-Y	82	64	19.0
Co(III)-Y	430	77	24.4
Cu(II)-Y	100	70	19.0
Fe(III)-Y	248	69	16.8
Cu-Pd-Y	160	72	34.3
Cu-Ni-Y	130	61	24.5
Cu-Fe-Y	150	68	31.2
Cu-Co-Y	190	78	21.4

The relation between the catalytic activity of Cu(II)-Y and the degree of Cu(II) exchange was examined at 120°C. The linear relation obtained in Fig. 3 is in contrast to the cases of olefin oxidation (*6*) and hydrocarbon cracking (*7*) over metal ion exchanged zeolite catalysts, where the catalytic activities have been reported to appear only when the metal ion content exceeds a certain exchange level. In these cases, it is understood that metal ions are located preferably at inactive sites at the lower exchange level. Y type zeolite has several cation sites in its unit cell, in such places as the hexagonal prism (site I), β-cage (I′ and II′) and supercage (II, III, etc.). Of these sites, site I and probably sites I′ and II′ are unfavorable in the catalysis because the space of the site itself or the cavity aperture leading to it is conceivably too narrow. According to Gallezot *et al.* (*8*), in the dehydrated Cu(II)-Y of 57% exchange, Cu(II) ions are located at sites I and I′. However, upon hydration of the zeolite or complexation of the metal

TABLE 2

The Promoting Effect of Co-exchanged Metal

Catalyst system	Sp act of Cu[a]	Redox potential (V)			
Cu–Co–Y	5.4	Co^{2+}/Co^{3+}	1.82	$Co(NH_3)_6^{2+}/Co(NH_3)_6^{3+}$	0.11
Cu–Pd–Y	2.9	Pd/Pd^{2+}	0.99	—	—
Cu–Fe–Y	2.4	Fe^{2+}/Fe^{3+}	0.77	—	—
Cu–Ni–Y	1.5	Ni/Ni^{2+}	−0.25	$Ni/Ni(NH_3)_6^{2+}$	−0.47
Cu–Y	1	Cu^{+}/Cu^{2+}	0.15	$Cu(NH_3)_2^{+}/Cu(NH_3)_4^{2+}$	−0.01

[a] Measured at the temperature of maximum activity (ca. 120°C) and represented relative to Cu–Y.

ion, the distribution of cations is likely to be changed in such a manner that more cations occupy the sites in the larger cavities. In the present study, the catalysts were kept at relatively low temperatures in the presence of NH_3 and H_2O. Hence, Cu(II) ions are considered to be situated in supercages to a considerable amount even at low exchange levels, giving rise to the linear correlation in Fig. 3.

In this connection, interesting are the reports (*9–12*) that NH_3 is adsorbed on Cu(II) exchanged in Y type zeolite to form a square planar complex $Cu(NH_3)_4^{2+}$ in the supercage at low temperatures. It has also been reported that the complete removal of NH_3 from the complex results in the migration of Cu(II) ions from the supercage to the β-cage (*13*). Considering these facts, it is possible that the bell-shaped correlation is coupled with such a cation migration in the zeolite. However, we think it more plausible that the correlation is associated with the change of the oxidation state of Cu as mentioned above.

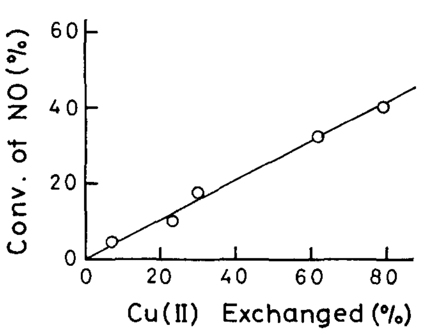

FIG. 3. Relation of the catalytic activity of Cu(II)–Y to the exchange level of Cu(II).

Catalytic Reaction over (Me_1, Me_2)–*Y*

Another interesting phenomenon was observed when binary metal ion exchanged Y zeolites, (Me_1, Me_2)–Y, were used. The catalytic activity–temperature profiles are shown in Fig. 4, where one component is fixed as Cu(II). The profiles are substantially the superpositions of those on the single metal ion exchanged zeolites. Quantitatively, however, additional promoting effects in catalytic activity were apparent in some of the binary systems. For example, [Cu(II), Fe(III)]–Y exhibited, at the temperature of the maximum activity, a specific activity per Cu(II) 2.4 times as high as that expected from the single component systems. Table 2 shows the relative specific activity of Cu(II) when promoted by the second components. The effect decreases in the order Co > Pd > Fe > Ni. Since this sequence coincides with the order of the standard redox potential of the metal ions, as shown in Table 2, it is conceivable that the coexisting metal ion participates in the catalysis as a redox system to alter the Cu(II)/Cu(I) ratio, though the promoting effect of Ni is difficult to account for in the same way. From Fig. 4, it is evident that

Cu(II) also promotes the catalytic action of other metal ions.

Mechanism of the NO–NH_3 Reaction over Cu(II)–Y

In order to elucidate the mechanism of the NO–NH_3 reaction over Cu(II)–Y, experiments were performed on the adsorption of the reactant gases as well as on the reaction kinetics.

Figure 5 shows the progress of adsorption of NH_3 and NO with time. A considerable amount of NH_3 was adsorbed on unexchanged zeolite, Na–Y, while with Cu(II)–Y rapid adsorption on Cu(II) ions occurred additionally. In contrast, NO adsorption was slow on Cu(II)–Y and was negligibly small on Na–Y. The amounts of adsorbed NH_3 and NO at saturation are shown in Fig. 6 for various partial pressures. In the case of NH_3, a net amount of adsorption on Cu(II) was obtained from the difference between Cu(II)–Y and Na–Y. This gave the average number of adsorbed NH_3 per Cu(II) equal to 2.5–4 at 25°C and 1.7–2.5 at 110°C, depending on the Cu(II) exchange level and the partial pressure of NH_3. Flentge *et al.* (*11*) have demonstrated that the ratio NH_3/Cu(II) becomes 4 to form the tetra-ammine complex at lower exchange levels but that at higher exchange levels the ratio deviates from 4 to a smaller one due to the increase of Cu(II) ions locating at sites unfavorable for complex formation.

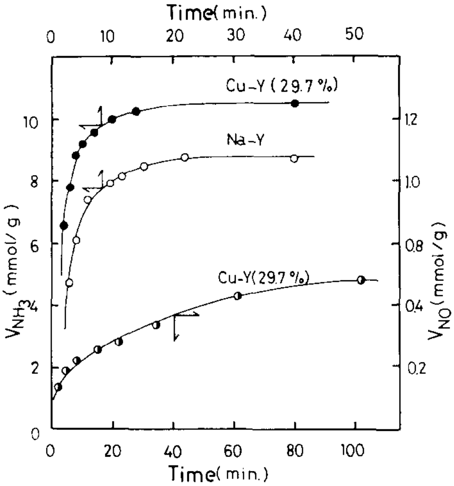

FIG. 5. Time courses of adsorption of NH_3 and NO over Cu(II)–Y and Na–Y (25°C).

In the case of NO adsorption, the observed NO/Cu(II) ratio was about unity (0.8–1.3). This coincides with the reports (*14*) that the ratio NO/metal becomes unity in NO adsorption over Fe_2O_3, NiO, Cr_2O_3 and Pt black. However, it is to be noted that the adsorption of NO in the present case was irreversible, i.e., the evacuation had little effect on the desorption. In

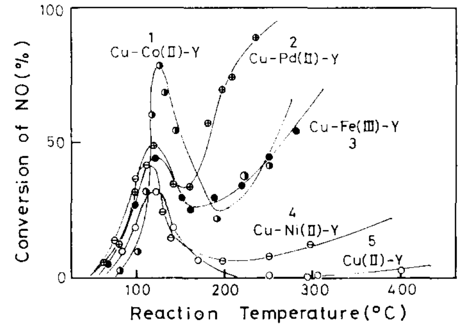

FIG. 4. Catalytic activity of (Cu(II), Me_2)–Y for the NO–NH_3 reaction. (1) Cu(II), 31%; Co(II), 62%; (2) Cu(II), 32%; Pd(II), 21%; (3) Cu(II), 36%; Fe(III), 62%; (4) Cu(II), 58%; Ni(II), 38%; (5) Cu(II), 68%.

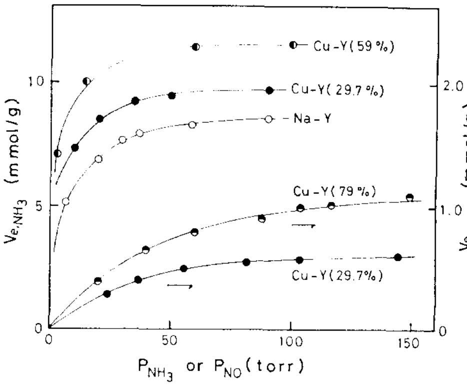

FIG. 6. Adsorption of NH_3 and NO over zeolite catalysts (25°C).

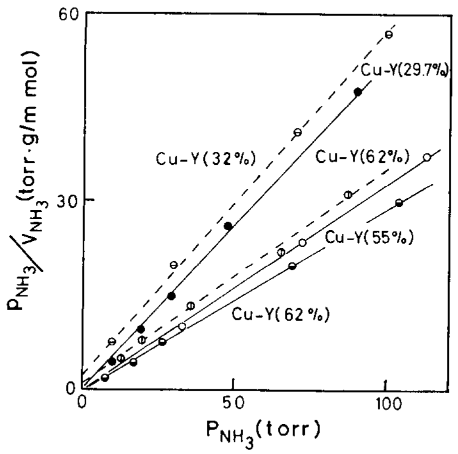

FIG. 7. Langmuir plots for isotherms of NH_3 adsorption on Cu(II).

this respect, Kasai and Bishop (*15*) reported that Cu(II) exchanged in Y zeolite undergoes an electron transfer reaction with adsorbed NO, being reduced to Cu(I).

The isotherm for NH_3 was expressed by the Langmuir equation,

$$V_e = \frac{SKP}{1 + KP} \quad \text{or} \quad \frac{P}{V_e} = \frac{P}{S} + \frac{1}{SK}, \qquad (1)$$

where V_e is the adsorbed amount in equilibrium; P, the partial pressure of adsorbate; K, the adsorption equilibrium constant; and S, the total number of adsorbent sites. P/V_e is plotted vs P in Fig. 7. In Fig. 7, the V_e values are for the net amount of NH_3 adsorbed on Cu(II) ions. The straight lines intercept near the origin, suggesting large K values. K is immeasurably large at 25°C, whereas it is 260–360/atm at 110°C.

Figure 8 shows the dependence of the rate of the NO–NH_3 reaction upon the partial pressures of reactant gases, P_{NO} and P_{NH_3}, at 110°C. The reaction order was unity in P_{NO} and 0.3–0.5 in P_{NH_3}. This was also the same at 140°C. The experimental rate equation was thus:

$$r = -\frac{dP_{NO}}{dt} = k_0 P_{NO} P_{NH_3}{}^{0.3-0.5}, \qquad (2)$$

where k_0 is an empirical rate constant. This suggests that the reaction sites are dominantly occupied by NH_3 in preference to NO.

On the basis of these experimental results on the adsorption and the kinetics, we tentatively propose that the NO–NH_3 reaction occurs between NO and NH_3 molecules coordinated to Cu(II) ions.

$$NH_3 + \text{Cu(II)-Y} \rightleftharpoons NH_3\cdots\text{Cu(II)-Y}, \qquad (3)$$

$$NO + \text{Cu(II)-Y} \rightleftharpoons NO\cdots\text{Cu(II)-Y}, \qquad (4)$$

$$NH_3\cdots\text{Cu(II)-Y} + NO\cdots\text{Cu(II)-Y} \rightarrow \text{products}. \qquad (5)$$

For the Langmuir–Hinshelwood type of reaction, the following rate equation is derived.

$$r = -\frac{dP_{NO}}{dt} = \frac{kK_{NO}K_{NH_3}P_{NO}P_{NH_3}}{(1 + K_{NO}P_{NO} + K_{NH_3}P_{NH_3})^2}, \qquad (6)$$

where k is the rate constant. Considering that $K_{NO}P_{NO} \ll K_{NH_3}P_{NH_3}$ in the present case, Eq. (6) is simplified to Eq. (7).

$$r = kK_{NO}K_{NH_3}P_{NO}P_{NH_3}/(1 + K_{NH_3}P_{NH_3})^2. \qquad (7)$$

Equation (7) satisfies the first order in NO experimentally found. To examine the

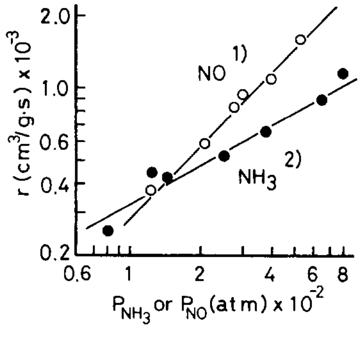

FIG. 8. Dependence of the rate of NO–NH_3 reaction on the partial pressures of NO at P_{NH_3} = 0.002 atm (1) and of NH_3 at P_{NO} = 0.03 atm (2) (110°C). Catalyst Cu(II)-Y (62%).

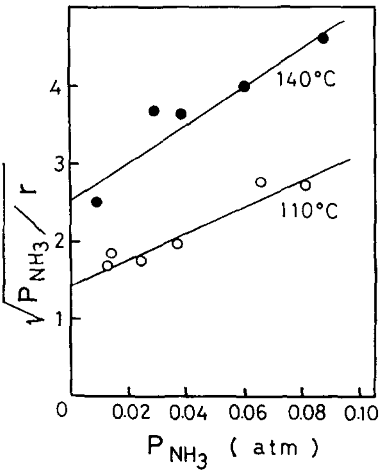

FIG. 9. Verification of the rate equation (8).

dependence on P_{NH_3}, Eq. (7) is transformed to Eq. (8).

$$(P_{NH_3}/r)^{\frac{1}{2}} = k'(1 + K_{NH_3}P_{NH_3}),$$
$$k' = (kK_{NO}K_{NH_3}P_{NO}). \qquad (8)$$

As shown in Fig. 9, Eq. (8) was verified by the linear plots of $(P_{NH_3}/r)^{\frac{1}{2}}$ against P_{NH_3} under the condition P_{NO} = constant. The value of K_{NH_3} deduced from Eq. (8) was, however, about one-fifth as large as the one obtained from the previous adsorption isotherm. The cause of this discrepancy is under examination.

In the reaction scheme (3), (4), and (5), it is highly probable that NO and NH_3 coordinate to common Cu(II) ions. This is especially so when one takes into account the linear dependence of the reaction rate on the exchange level of Cu(II). In fact, such a complex has been proposed by Lunsford *et al.* in the esr study of Co(II)-Y exposed to NH_3 and NO. In this case, however, the catalyst was reported to suffer irreversible change soon after the exposure to the gases, in agreement with our results mentioned before.

The reaction scheme proposed above is concerned only with the rate determining step. The reaction path leading to the final products, N_2, N_2O, and H_2O seems to be very complex. Further studies are in progress.

REFERENCES

1. Shelef, M., and Gandhi, H., *Ind. Eng. Chem. Process Design Develop.* **11**, 393 (1972).

2. Kobylinski, T. P., and Taylor, B. W., *J. Catal.* **33**, 376 (1974).

3. Shelef, M., Otto, K., and Gandhi, H., *J. Catal.* **12**, 361 (1968).

4. Kasaoka, S., Tsumaki, H., and Kitamura, T., *Nippon Kagaku Kaishi* **1973**, 1052.

5. Echigoya, E., Niiyama, H., and Ebitani, A., *Nippon Kagaku Kaishi,* **1974**, 222.

6. Mochida, I., Jitsumatsu, T., Kato, A., and Seiyama, T., *J. Catal.* **36**, 361 (1975).

7. Minachev, K. M., *Kinet. Katal.* **11**, 412 (1970).

8. Gallezot, P., Taarit, Y. B., and Imelik, B., *C. R. Acad. Sci., Ser. C* **272**, 261 (1971); *J. Catal.* **26**, 481 (1972).

9. Vansant, E. F., and Lunsford, J. H., *J. Phys. Chem.* **76**, 2860 (1972).

10. Huang, Y.-Y., and Vansant, E. F., *J. Phys. Chem.* **77**, 663 (1973).

11. Flentge, D. R., Lunsford, J. H., Jacobs, P. A., and Uytterhoeven, J. B., *J. Phys. Chem.* **79**, 354 (1975).

12. Windhorst, K. A., and Lunsford, J. H., *J. Amer. Chem. Soc.* **97**, 1407 (1975).

13. Naccache, C., and Taarit, Y. B., *Chem. Phys. Lett.* **11**, 11 (1971).

14. Otto, K., and Shelef, M., *J. Catal.* **14**, 226 (1969); **18**, 184 (1970); **29**, 138 (1973); Gandhi, H. S, and Shelef, M., *J. Catal.* **24**, 241 (1972).

15. Kasai, P. H., Bishop, R. J., Jr., *J. Phys. Chem.* **77**, 2308 (1973).

16. Williamson, W. B., Flentge, F. R., and Lunsford, J. H., *J. Catal.* **37**, 258 (1975).

17. Herman, R. G., Lunsford, J. H., Beyer, H., Jacobs, P. A., and Uytterhoeven, J. B., *J. Phys. Chem.* **79**, 2388 (1975).